


# Large-Scale Meta-Analysis of Human Medial Frontal Cortex Reveals Tripartite Functional Organization

Alejandro de la Vega,<sup>1,2</sup>  Luke J. Chang,<sup>3</sup> Marie T. Banich,<sup>1,2</sup>  Tor D. Wager,<sup>1,2</sup> and  Tal Yarkoni<sup>4</sup>

<sup>1</sup>Department of Psychology and Neuroscience and <sup>2</sup>Institute of Cognitive Science, University of Colorado, Boulder, Colorado 80309, <sup>3</sup>Department of Psychological and Brain Sciences, Dartmouth College, Hanover, New Hampshire 03755, and <sup>4</sup>Department of Psychology, University of Texas, Austin, Texas 78712

The functional organization of human medial frontal cortex (MFC) is a subject of intense study. Using fMRI, the MFC has been associated with diverse psychological processes, including motor function, cognitive control, affect, and social cognition. However, there have been few large-scale efforts to comprehensively map specific psychological functions to subregions of medial frontal anatomy. Here we applied a meta-analytic data-driven approach to nearly 10,000 fMRI studies to identify putatively separable regions of MFC and determine which psychological states preferentially recruit their activation. We identified regions at several spatial scales on the basis of meta-analytic coactivation, revealing three broad functional zones along a rostrocaudal axis composed of 2–4 smaller subregions each. Multivariate classification analyses aimed at identifying the psychological functions most strongly predictive of activity in each region revealed a tripartite division within MFC, with each zone displaying a relatively distinct functional signature. The posterior zone was associated preferentially with motor function, the middle zone with cognitive control, pain, and affect, and the anterior with reward, social processing, and episodic memory. Within each zone, the more fine-grained subregions showed distinct, but subtler, variations in psychological function. These results provide hypotheses about the functional organization of medial prefrontal cortex that can be tested explicitly in future studies.

**Key words:** cognitive control; medial frontal cortex; meta-analysis; pain

## Significance Statement

Activation of medial frontal cortex in fMRI studies is associated with a wide range of psychological states ranging from cognitive control to pain. However, this high rate of activation makes it challenging to determine how these various processes are topologically organized across medial frontal anatomy. We conducted a meta-analysis across nearly 10,000 studies to comprehensively map psychological states to discrete subregions in medial frontal cortex using relatively unbiased data-driven methods. This approach revealed three distinct zones that differed substantially in function, each of which were further subdivided into 2–4 smaller subregions that showed additional functional variation. Each individual region was recruited by multiple psychological states, suggesting subregions of medial frontal cortex are functionally heterogeneous.

## Introduction

The medial frontal cortex (MFC) is purported to play a key role in a number of psychological processes, including motor function, cognitive control, emotion, pain, and social cognition. However,

the precise correspondence of psychological states onto discrete medial frontal anatomy remains elusive. Several recent attempts to define distinct functional subregions of MFC have been based on morphology (Palomero-Gallagher et al., 2013; Vogt, 2016), *in vivo* structural connectivity (Johansen-Berg et al., 2004; Beckmann et al., 2009; Sallet et al., 2013; Neubert et al., 2014), and functional connectivity (Andrews-Hanna et al., 2010). Although such studies map key properties that constrain information processing in MFC, it is unclear whether these boundaries correspond to patterns of brain activity observed during behavioral performance (Eickhoff et al., 2007; Amunts and Zilles, 2015; Mattar et al., 2015). Moreover, as these methods do not measure the brain's response to various psychological challenges, they cannot directly identify the (potentially separable) functional associates of MFC subregions.

Received Dec. 8, 2015; revised May 13, 2016; accepted May 14, 2016.

Author contributions: A.d.l.V., M.T.B., T.D.W., and T.Y. designed research; A.d.l.V. and T.Y. performed research; L.J.C. and T.Y. contributed unpublished reagents/analytic tools; A.d.l.V., L.J.C., and T.Y. analyzed data; A.d.l.V., L.J.C., M.T.B., T.D.W., and T.Y. wrote the paper.

This work was supported by National Institutes of Health Grant R01MH096906.

The authors declare no competing financial interests.

Correspondence should be addressed to Dr. Alejandro de la Vega, Department of Psychology and Neuroscience, University of Colorado Boulder, Muenzinger D244, 345 UCB, Boulder, CO 80309-0345. E-mail: delavega@colorado.edu.

DOI:10.1523/JNEUROSCI.4402-15.2016

Copyright © 2016 the authors 0270-6474/16/366553-10\$15.00/0

To this end, task-based fMRI has suggested that distinct foci of MFC activation may be associated with specific psychological manipulations. For example, the supplementary motor area (SMA) and pre-SMA have been associated with the planning and initiation of movements (Roland et al., 1980; Kennerley et al., 2004; Leek and Johnston, 2009), whereas midcingulate cortex (MCC) has been implicated in various aspects of cognitive control (Botvinick et al., 1999; Milham et al., 2001; Holroyd et al., 2004; Brown and Braver, 2005; Shenhav et al., 2013), fear (Vogt and Vogt, 2003; Milad et al., 2007; Etkin et al., 2011), and pain processing (Rolls et al., 2003; Wager et al., 2013; Vogt, 2016). Further, anterior, medial prefrontal cortex (mPFC), and the rostral anterior cingulate cortex (rACC) have been associated with affective processes, including emotion (Etkin et al., 2011; Lindquist et al., 2012), autonomic function (Critchley et al., 2003), and valuation (Hare et al., 2009), as well as internally oriented processes, such as mentalizing (Baumgartner et al., 2012) and autobiographical memory (Spreng and Grady, 2010).

Despite the large number of neuroimaging studies, there have been few large-scale efforts to comprehensively map the full range of psychological functions onto medial frontal anatomy. Most meta-analyses are restricted to a subset of empirical findings relevant to candidate cognitive states hypothesized to be important (e.g., negative affect, pain, cognitive control) (Shackman et al., 2011) or a specific anatomical region of interest (e.g., Palomero-Gallagher et al., 2015). This relatively narrow scope limits the ability to address the specificity of activation of psychological states across the MFC more broadly. That is, without considering a wide representative range of psychological states, it is difficult to determine whether particular psychological processes preferentially recruit specific subdivisions of MFC. This limitation, widely known as the reverse inference problem (Poldrack, 2006), is particularly acute for portions of MFC, which commonly activate in a large proportion of fMRI studies, raising questions about whether these regions are selectively involved in specific mental functions (Nelson et al., 2010; Yarkoni et al., 2011).

Here we address these issues by creating a comprehensive mapping between psychological states and MFC anatomy using Neurosynth (Yarkoni et al., 2011), a framework for large-scale fMRI meta-analysis composed of nearly 10,000 studies. We first clustered MFC voxels into functionally separable regions at several spatial scales based on their coactivation across studies with the rest of the brain (Kober et al., 2008; Toro et al., 2008; Smith et al., 2009; Robinson et al., 2010). In contrast to cytoarchitectonic and connectivity-based parcellations, the present analysis identified clusters with distinct signatures of activation across a wide range of psychological manipulations. This procedure revealed three zones along the rostrocaudal axis that further fractionated into nine subregions. We then characterized each cluster's functional profiles using multivariate classification, revealing broad functional shifts between the three zones, and subtler variations between their corresponding subregions. Collectively, our results provide a comprehensive functional map of the human MFC using relatively unbiased data-driven methods.

## Materials and Methods

We analyzed version 0.4 of the Neurosynth database (Yarkoni et al., 2011), a repository of 9721 fMRI studies and >350,000 activation peaks that span the full range of the published literature. The studies included human subjects of either sex. Each observation contains the peak activations for all contrasts reported in a study's table as well as the frequency of all of the words in the article abstract. A heuristic but relatively accurate approach is used to detect and convert reported coordinates to the standard MNI space (Yarkoni et al., 2011). As such, all activations and

subsequent analyses are in MNI152 coordinate space. The scikit-learn Python package (Pedregosa et al., 2011) was used for all machine learning analyses. Analyses were performed using the core Neurosynth Python tools (<https://github.com/neurosynth/neurosynth>); code and data to replicate these analyses on any given brain region at any desired spatial granularity are available as a set of IPython Notebooks (<https://github.com/adelavega/neurosynth-mfc>).

**Coactivation-based clustering.** We clustered individual voxels inside an MFC mask based on their meta-analytic coactivation with voxels in the rest of the brain (Fig. 1A). First, we defined an MFC mask, excluding voxels further than 10 mm from the midline of the brain, posterior to the central sulcus ( $Y < -22$  mm) and ventral to ventromedial PFC (vmPFC;  $Z < -32$  mm). Next, we removed voxels with low gray matter signal by excluding voxels with either <30% probability of gray matter cortex according to the Harvard-Oxford (H-O) anatomical atlas or very low activation rates in the database (<80 studies per voxel). In general, Neurosynth's activation mask (derived from the standard MNI152 template distributed with FSL) corresponded highly with probabilistic locations of cerebral cortex, with the exception of portions of precentral gyrus and far vmPFC, which showed low activation, although they were >50% likely to be in cerebral cortex.

Next, we calculated the coactivation of each MFC voxel with the rest of the brain by correlating the target voxel's activation pattern across studies with the rest of the brain. Activation in each voxel is represented as a binary vector of length 9721 (the number of studies). A value of 1 indicated that the voxel fell within 10 mm of an activation focus reported in a particular study, and a value of 0 indicated that it did not. Because correlating the activation of every MFC voxel with every other voxel in the brain would result in a very large matrix (15,259 MFC voxels  $\times$  228,453 whole-brain voxels) that would be computationally costly to cluster, we reduced the dimensionality of the whole brain to 100 components using principal components analysis (PCA; the precise choice of number of components does not materially affect the reported results). Next, we computed the Pearson correlation distance between every voxel in the MFC mask with each whole-brain PCA component. We applied *k*-means clustering to this matrix (15,259 MFC voxels  $\times$  100 whole-brain PCA components) to group the MFC voxels into 2–15 clusters. *k*-means was used for clustering as this algorithm is computationally efficient, is widely used, and shows reasonably high goodness-of-fit characteristics (Thirion et al., 2014). We used the *k*-means<sup>++</sup> initialization procedure, ran the algorithm 10 times on different centroid seeds, and selected the output of these consecutive runs with the lowest inertia to avoid local minima.

Because the optimality of a given clustering depends in large part on investigators' goals, the preferred level of analysis, and the nature and dimensionality of the available data, identifying the "correct" number of clusters is arguably an intractable problem (Varoquaux and Thirion, 2014; Eickhoff et al., 2015; Poldrack and Yarkoni, 2016). However, in the interest of pragmatism, we attempted to objectively select the number of clusters using the silhouette score, a measure of within-cluster cohesion. The silhouette coefficient was defined as  $(b - a)/\max(a, b)$ , where *a* is the mean intracluster distance and *b* is the distance between a sample and the nearest cluster of which the sample is not a part. Solutions that minimized the average distance between voxels within each cluster received a greater score. To estimate the uncertainty around silhouette scores, we used a permutation procedure previously used by our group (Wager et al., 2008).

To understand the anatomical correspondence of the resulting clusters, we calculated the probability of voxels in each cluster occurring in probabilistic regions from the H-O atlas. We refer to H-O's Juxtapositional Lobule Cortex as SMA for consistency. We also compared the location of clusters to regions from cytoarchitectonic atlases of medial motor areas (Picard and Strick, 1996), MCC (Vogt, 2016), and vmPFC (Mackey and Petrides, 2014). To be precise, subregions in the 9-cluster solution were given alphanumeric labels in addition to descriptive names.

**Coactivation profiles.** Next, we analyzed the differences in whole-brain coactivation between the resulting clusters (Fig. 1B). To highlight differences between clusters, we contrasted related sets of clusters. For the three-cluster solution, we contrasted the coactivation of each cluster

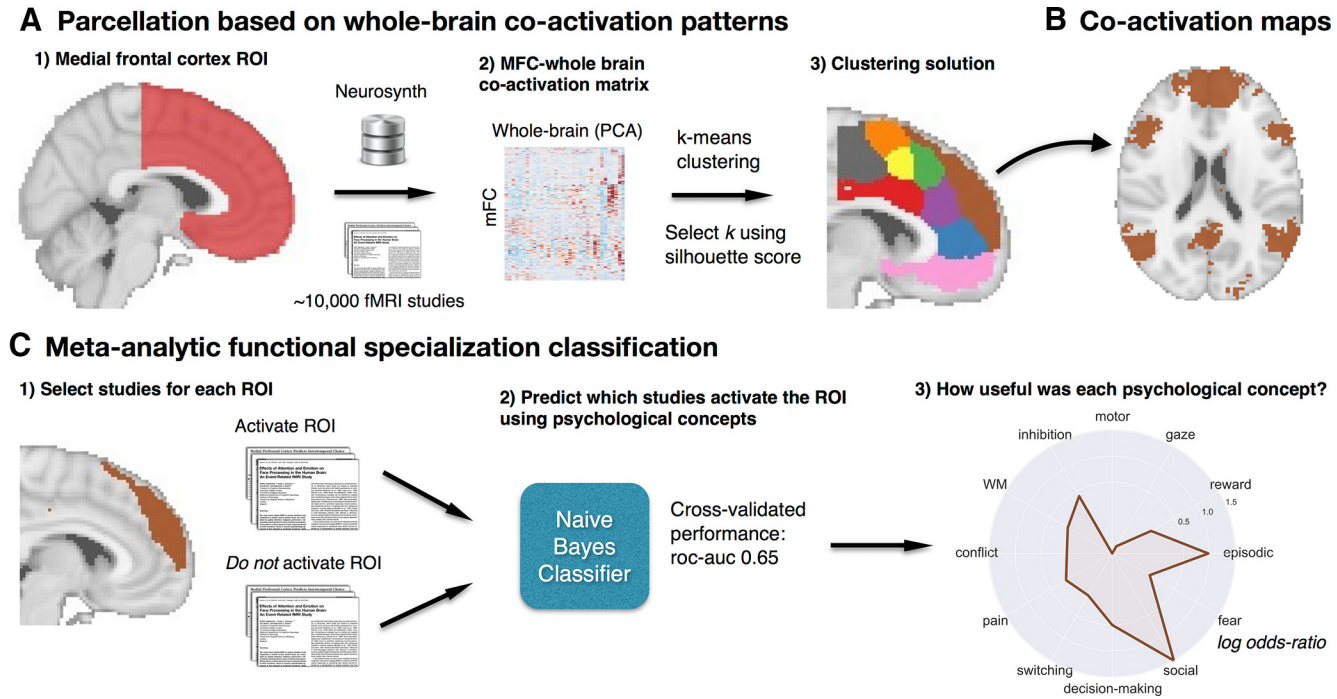


**Figure 1.** Methods overview. **A**, Whole-brain coactivation of MFC voxels was calculated, and *k*-means clustering was applied, resulting in spatially distinct clusters. **B**, For each cluster, thresholded whole-brain coactivation maps were generated. **C**, We generated functional preference profiles for each cluster by determining which psychological topics best predicted their activation.

(e.g., “posterior zone”) with the other two clusters (e.g., “middle” and “anterior” zones). For the 9-cluster solution, we contrasted the coactivation of each cluster (e.g., “SMA”) with spatially adjacent clusters that fell within the same zone of the three-cluster solution (e.g., “pre-SMA”). To do so, we performed a meta-analytic contrast between studies that activated a given cluster and studies that activated control clusters. The resulting images identify voxels with a greater probability of coactivating with the cluster of interest than with control clusters. For example, voxels in Figure 3*B* (first panel, gray) indicate voxels that are active more frequently in studies in which SMA (P1) is active than in studies in which pre-SMA (P2) is active. We calculated *p* values for each voxel using a two-way  $\chi^2$  test between the two sets of studies and thresholded the coactivation images using the False Discovery Rate ( $q < 0.01$ ). The resulting images were binarized for display purposes and visualized using the Nilearn library for Python.

**Topic modeling.** Although term-based meta-analysis maps in Neurosynth often approximate the results of manual meta-analyses of the same concepts, there is a high degree of redundancy between terms (e.g., “episodes” and “episodic”), as well as potential ambiguity as to the meaning of an individual word out of context (e.g., “memory” can indicate working memory [WM] or episodic memory). To remedy this problem, we used a reduced semantic representation of the latent conceptual structure underlying the neuroimaging literature: a set of 60 topics derived using latent dirichlet allocation topic modeling (Blei et al., 2003). This procedure was identical to that used in a previous study (Poldrack et al., 2012a), except for the use of a smaller number of topics and a much larger version of the Neurosynth database. The generative topic model derives 60 independent topics from the co-occurrence across studies of all words in the abstracts fMRI studies in the database. Each topic loads onto individual words to a varying extent, facilitating the interpretation of topics; for example, a WM topic loads highest on the words “memory, WM, load,” whereas an episodic memory topic loads on “memory, retrieval, events.” Both topics highly load on the word “memory,” but the meaning of this word is disambiguated because it is contextualized by other words that strongly load onto that topic. Of the 60 generated topics, we excluded 25 topics representing nonpsychological phenomena, such as the nature of the subject population (e.g., gender, special populations) and methods (e.g., words such as “images,” “voxels”), resulting in 35

**Table 1. Topics most strongly associated with MFC regions used in Figure 4<sup>a</sup>**

Topic name	Highest loading words
Gaze	Eye, gaze, movements, eyes, visual, saccades, saccade, target, fixation, direction
Decision-making	Decision, choice, risk, decisions, choices, uncertainty, outcomes, risky, taking, outcome
Episodic	Memory, events, imagery, autobiographical, retrieval, episodic, memories, future, mental, semantic
Motor	Motor, movement, movements, sensorimotor, primary, finger, control, imagery, tasks, force
Social	Social, empathy, moral, person, judgments, mentalizing, mental, theory, people, mind
Reward	Reward, anticipation, monetary, responses, rewards, motivation, motivational, loss, incentive, punishment
Switching	Cues, target, trials, cue, switching, stimulus, targets, preparation, switch, selection
Conflict	Conflict, interference, control, incongruent, trials, stroop, congruent, cognitive, behavioral, rt
Inhibition	Inhibition, control, inhibitory, stop, motor, trials, nogo, cognitive, suppression, aggression
Fear	Fear, anxiety, threat, responses, conditioning, cs, extinction, autonomic, conditioned, arousal
Working memory	Memory, performance, cognitive, WM, tasks, verbal, load, executive, test, maintenance
Pain	Pain, painful, stimulation, somatosensory, intensity, noxious, heat, nociceptive, placebo, chronic

<sup>a</sup>Ten strongest loading words for each topic are listed, in descending order of association strength.

psychological topics. See Table 1 for a list of topics most associated with MFC.

**Meta-analytic functional preference profiles.** We generated functional preference profiles by determining which psychological topics best predicted each MFC cluster’s activity across fMRI studies (Fig. 1*C*). First, we selected two sets of studies: studies that activated a given cluster, defined as activating at least 5% of voxels in the cluster; and studies that were not defined as activating no voxels in the cluster. For each cluster, we trained a naive Bayes classifier to discriminate these two sets of studies based on



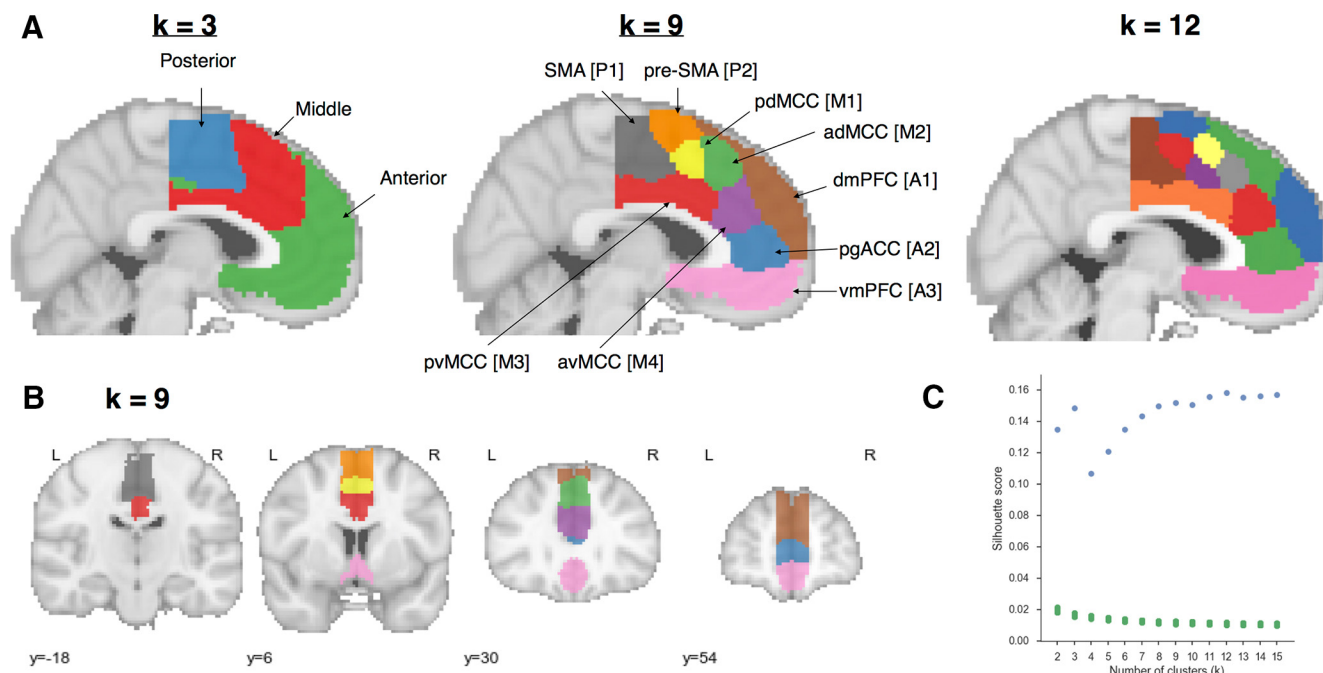


**Figure 2.** Coactivation-based clustering of MFC results. **A**, Mid-sagittal view at three levels at granularity: three broad zones, nine and 12 subregions. Clusters in nine subregion solution are given both descriptive and alphanumeric names for reference. **B**, Axial view of nine subregions. **C**, Silhouette scores of real (green) and permuted (blue) clustering solutions. Clustering was performed on permuted data 1000 times for each  $k$  to compute a null distribution ( $p$  values for all clusters  $< 0.001$ ). Silhouette scores reached local maxima at 3 regions and plateaued after 9.

psychological topics herein. We chose naive Bayes because (1) we have previously had success applying this algorithm to Neurosynth data (Yarkoni et al., 2011); (2) these algorithms perform well on many types of data (Androutsopoulos et al., 2000); (3) they require almost no tuning of parameters to achieve a high level of performance; and (4) they produce highly interpretable solutions, in contrast to many other machine learning approaches (e.g., support vector machines or decision tree forests).

We trained models to predict whether or not fMRI studies activated each cluster, given the semantic content of the studies. In other words, if we know which psychological topics are mentioned in a study, how well can we predict whether the study activates a specific region? We used fourfold cross-validation for testing and calculated the mean score across all folds as the final measure of performance. We scored our models using the area under the curve of the receiver operating characteristic (AUC-ROC), a summary metric of classification performance that takes into account both sensitivity and specificity. AUC-ROC was chosen because this measure is not detrimentally affected by unbalanced data (Jeni et al., 2013), which was important because each cluster varied in the ratio of studies that activated it to the studies that did not.

To generate preference profiles, we extracted from the naive Bayes models the log odds-ratio (LOR) of a topic being present in active studies versus inactive studies. The LOR was defined as the log of the ratio between the probability of a given topic in active studies and the probability of the topic in inactive studies, for each cluster individually. LOR values  $> 0$  indicate that a psychological topic is predictive of activation in a given cluster. To determine the statistical significance of these associations, we permuted the class labels and extracted the LOR for each topic 1000 times. This resulted in a null distribution of LOR for each topic and each cluster. Using this null distribution, we calculated  $p$  values for each pairwise relationship between psychological concepts and cluster, and reported associations significant at the  $p < 0.001$  threshold. Finally, to determine whether certain topics showed greater preference for one cluster versus another, we conducted exploratory, *post hoc* comparisons by determining whether the 95% CIs of the LOR of a specific topic for one cluster overlapped with the 95% CI of the same topic for another cluster. We generated CIs using bootstrapping, sampling with replacement, and recalculating log-odds ratios for each cluster 1000 times.

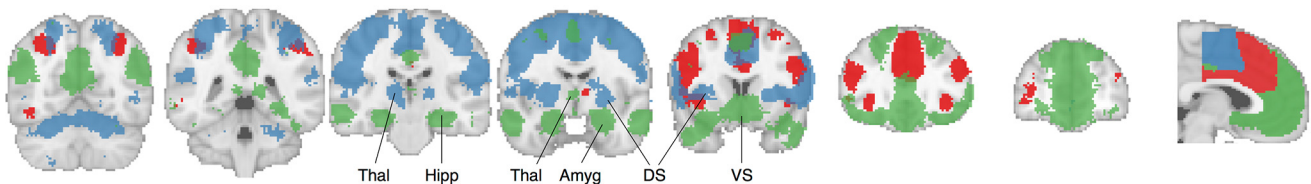
## Results

### Functionally separable regions of MFC

We identified spatially dissociable regions on the basis of shared coactivation profiles with the rest of the brain (Kober et al., 2008; Toro et al., 2008; Smith et al., 2009; Chang et al., 2013), an approach that exploits the likelihood of a voxel coactivating with another voxel across studies in the meta-analytic database (Fig. 2). Because structure-to-function mappings can be identified at multiple spatial scales, we iteratively extracted 2-cluster through 15-cluster solutions and assessed their validity using the silhouette score, a commonly used measure of intercluster coherence. Permutation analyses indicated that the null hypothesis of random clustering could be rejected for all solutions, with silhouette scores reaching local maxima at 3 clusters (Fig. 2C). The plateauing of silhouette scores suggests that there is little objective basis for selecting one solution over another past around 9 clusters (Thirion et al., 2014). We have therefore opted to focus on the 3-cluster and 9-cluster solutions because they provide greater theoretical parsimony than more fine-grained solutions. We henceforth refer to the clusters from the 3-cluster solution as “zones” to differentiate them from clusters in the 9-cluster solution, which we refer to as “subregions.”

At the coarsest level, MFC divided into three broad bilateral clusters organized along the rostrocaudal axis. The 9-cluster solution revealed additional fine-grained topographical organization, with each of the three zones fractionating into 2–4 smaller regions (84% of all voxels within each zone overlapped with its putative subregions). To better understand the anatomical location of our clusters, we compared them with previously defined subregions from the H-O probabilistic structural atlas and well-known cytoarchitectonic studies. Although we did not necessarily expect our clusters to conform precisely to morphologically derived regions, we nonetheless observed moderate correspon-

## A Functional zones



## B Sub-regions

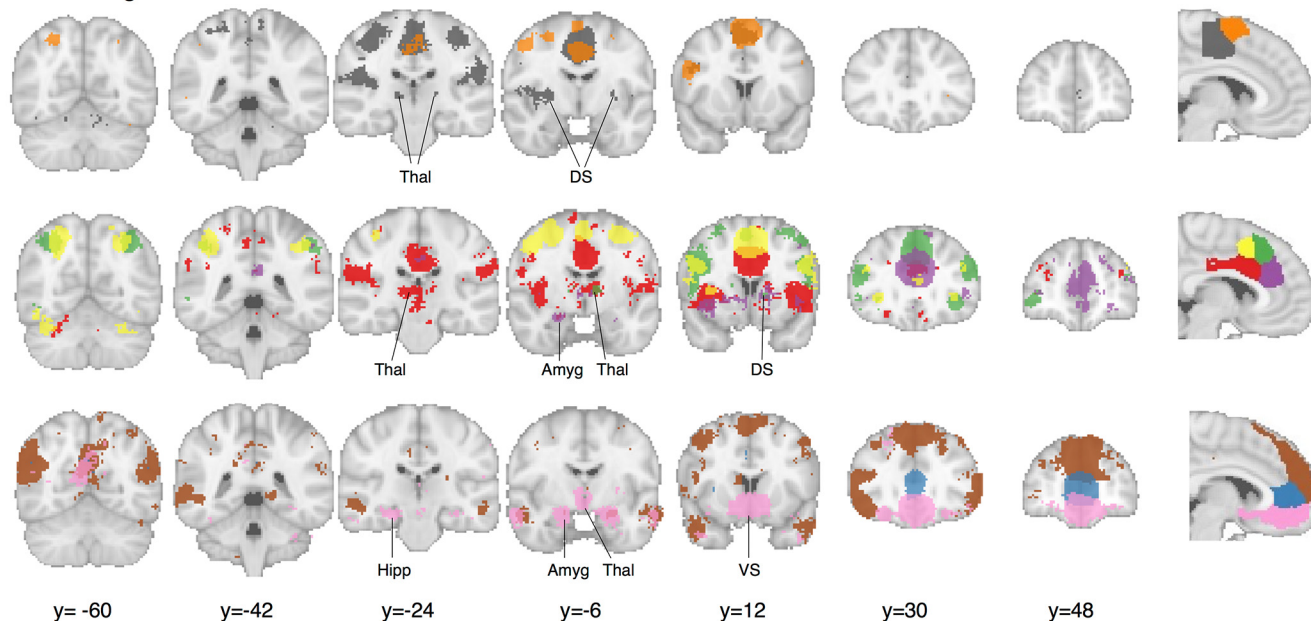


**Figure 3.** Meta-analytic coactivation contrasts for (**A**) three zones and (**B**) nine subregions. Colored voxels indicate significantly greater coactivation with the seed region of the same color (at right) than control regions in the same row. The three zones showed distinct coactivation patterns, whereas subregions within each zone showed fine-grained coactivation differences. Images are presented using neurological convention and were whole-brain corrected using a false discovery rate of  $q = 0.01$ . Major subcortical structures are labeled as follows: Thal, Thalamus; Hipp, hippocampus; Amyg, amygdala; VS, ventral striatum; DS, dorsal striatum.

dence, suggesting that morphological properties constrain, but not determine, function. Within the posterior zone, we identified two clusters (Fig. 2A; SMA [P1] and pre-SMA [P2]) with a high probability of occurring in SMA according to H-O. The two clusters were approximately delineated by the vertical commissure anterior, consistent with cytoarchitectonic delineations (Picard and Strick, 1996). However, SMA (P1) spanned multiple cytoarchitectonic areas, extending ventrally to include portions of Picard and Strick's cingulate zones, suggesting that these morphologically distinct areas coactivate similarly across tasks.

In the middle zone, we identified four clusters consistent with MCC. In particular, two anterior and two posterior clusters delineated from each other a few millimeters anterior to the vertical commissure anterior, consistent with Vogt's definition of anterior and posterior midcingulate cortex (Vogt, 2016). The two dorsal clusters (pdMCC [M1] and adMCC [M2]) showed a high probability of falling within H-O's paracingulate gyrus, whereas the two ventral clusters (pvMCC [M3] and avMCC [M4]) showed a high probability of falling in the cingulate gyrus proper. Unlike some cytoarchitectonic studies, we did not identify any regions exclusively located in the cingulate sulcus, such as the rostral cingulate zone.

In the anterior zone, the most dorsal cluster (dorsal medial PFC [dmPFC], A1) included medial aspects of H-O's frontal pole and superior frontal gyrus and was entirely outside of the anterior cingulate gyrus. Ventrally, we identified a second cluster (pre-

genual anterior cingulate cortex [pgACC], A2), which was primarily located within pregenual aspects of the anterior cingulate gyrus but also included pregenual portions of paracingulate gyrus. Finally, the most ventral cluster (vmPFC, A3) encompassed both pregenual aspects of the ACC and medial OFC, similar to the vmPFC area of interest used in cytoarchitectonic studies (Mackey and Petrides, 2014).

Next, to provide direct insight into the functions of the clusters we identified, we applied two approaches. First, we determined which other brain regions coactivate with each cluster, to reveal their functional networks. Second, we used semantic data from Neurosynth to determine which psychological states predict the activation of each cluster.

### Meta-analytic coactivation profiles

We directly contrasted coactivation patterns of the three functional zones (i.e., we sought to identify voxels that coactivated to a stronger degree with each zone than with the other two) (Fig. 3A). The posterior zone showed greater bilateral coactivation with the primary motor cortex (PMC), superior parietal cortex (SPC), anterior cerebellum, and posterior insula (pIns) as well subcortical regions, such as the thalamus and dorsal striatum (DS), a coactivation pattern consistent with motoric function. The middle zone coactivated with anterior aspects of the thalamus as well as regions in the frontoparietal control network, such as dorsolateral prefrontal cortex (DLPFC), anterior insula (aIns),

and SPC. Finally, the anterior zone showed a qualitatively different pattern, coactivating to a greater extent with default network regions, such as angular gyrus, hippocampus, and posterior cingulate cortex (PCC) (Andrews-Hanna, 2012). The anterior zone also showed greater coactivation with subcortical regions important for affect: the amygdala and ventral striatum (VS).

To understand the differences in coactivation found within each zone, we directly contrasted the coactivation patterns of each zone's subregions (Fig. 3B). In the posterior zone, SMA (P1) showed greater coactivation with somatosensory cortices and pIns, whereas pre-SMA (P2) showed greater coactivation with posterior DLPFC, including the inferior frontal junction (IFJ), as well as aIns, regions associated with goal-directed cognition (Nelson et al., 2010; Chang et al., 2013). Within the middle zone, we found that all four subregions strongly coactivated with various aspects of the insula. However, pvMCC (M3) more strongly coactivated with pIns, SII, and the brainstem, important regions for pain processing (Vogt, 2005; Wager et al., 2013). In contrast, avMCC (M4) coactivated more strongly with ventral aIns and lateral OFC, regions previously associated with reward-driven learning (Stalnaker et al., 2015), and both dorsal MCC (M1 and M2) clusters more strongly coactivated with dorsal aIns and frontoparietal control regions (e.g., DLPFC, SPC). However, adMCC (M2)'s coactivation extended anteriorly into the frontal pole, whereas pdMCC (M1) more strongly coactivated with motor cortices. Subcortically, pvMCC (M3) showed greater coactivation with the thalamus and DS, whereas avMCC (M4) showed greater coactivation with the left amygdala. However, daMCC (M2) also showed robust coactivation with portions of thalamus and DS.

Within the anterior zone, pgACC (A2) did not show many coactivation differences from its neighbors. Surprisingly, both dmPFC (A1) and vmPFC (V3) showed greater coactivation with PCC, a key default network region. In addition, dmPFC (A1) robustly coactivated with portions of the so-called "mentalizing" network, such as the tempoparietal junction (TPJ) (Carter and Huettel, 2013) and the superior temporal sulcus (STS) (Zilbovicius et al., 2006), as well as lateral PFC, including inferior and middle frontal gyri. Finally, vmPFC (A3) showed strong coactivation with subcortical regions, including VS and the amygdala, extending into the hippocampus. As a whole, these coactivation patterns demonstrate that the regions we identified are involved with distinct functional networks, and suggest that there are likely broad functional differences across MFC zones, accompanied by fine-grained differences between subregions.

### Meta-analytic functional preference profiles

Next, we used a data-driven approach that surveyed a broad range of psychological states to determine whether MFC clusters are differentially recruited by psychological states. For each cluster, we trained a multivariate classifier to predict which studies activated the cluster using a set of 35 psychological topics derived by applying a standard topic modeling approach to the abstracts of articles in the database (Poldrack et al., 2012b) (Table 1). From the resulting fitted classifiers, we calculated a measure of how strongly each topic indicated that a study activated a given cluster (measured as the LOR of the probability of a each topic in studies that activated a given cluster to the probability of the same topic in studies that did not activate the cluster). LOR values  $>0$  indicate that the presence of that topic in a study predicts activity in a given region. We restricted interpretation to significant associations ( $p < 0.001$ ) and additionally report 95% CIs of LORs whenever we comparatively discuss sets of regions. As the latter

comparisons are *post hoc* and exploratory, caution in interpretation is warranted.

Although the following results demonstrate relatively high loadings between specific topics and regions (e.g., "motor" and SMA), classification using all 35 topics yielded much better performance (mean AUC-ROC: 0.61) than when using only the most predictive topic of each region (mean AUC-ROC: 0.54). The relatively poor performance when using only one topic suggests low selectivity between psychological states and any one region.

Across the three broad MFC zones, we observed distinct functional patterns, consistent with their divergent patterns of functional coactivation (Fig. 3). The posterior zone was primarily involved with motor function (including gaze), consistent with its coactivation with motor regions. The middle zone was primarily associated with various facets of cognitive control but was also implicated in negative affect, pain, and fear, as well as decision-making. Consistent with its distinct pattern of coactivation, the anterior zone showed a robust shift away from goal-directed cognition and was strongly associated with affective processes, such as reward, fear, and decision-making, as well as internally oriented processes, such as episodic memory and social processing.

Inspection at a finer spatial scale revealed that subregions within each zone showed more subtle patterns of psychological function, similar to the fine-grained variations in coactivation previously observed for each subregion. In the posterior zone (Fig. 4, bottom left), activity in both clusters was similarly predicted by motor function and switching. However, exploratory *post hoc* tests suggested that SMA (P1) was more strongly associated with pain, whereas pre-SMA (P2) was more strongly associated with WM (95% CI LOR: pain: SMA [0.6, 1.1], pre-SMA [−0.1, 0.4]; WM: SMA [−0.2, 0.1], pre-SMA [0.2, 0.4]).

In the middle zone (Fig. 4, bottom middle), activity in all four subregions was significantly predicted by aspects of cognitive control (i.e., conflict and inhibition) and pain. However, *post hoc* exploratory tests indicated dorsal MCC (M1 and M2) was more strongly associated with WM than ventral MCC (M3 and M4) (95% CI LOR: pdMCC [0.5, 0.8], adMCC [0.4, 0.6], pvMCC [0, 0.15], avMCC [0, 0.3]), whereas ventral MCC showed a stronger association with affect (95% CI LOR: fear: pdMCC [−0.1, 0.4], adMCC [−0.4, 0.2], pvMCC [0.7, 1.2], avMCC [0.4, 0.9]; reward: pdMCC [−0.4, 0.1], adMCC [−0.4, 0.1], pvMCC [0.3, 0.7], avMCC [0.3, 0.8]; pain: pdMCC [0.3, 0.8], adMCC [0.2, 0.7], pvMCC [1.1, 1.5], avMCC [0.6, 1.1]). Finally, both anterior clusters showed a greater association with decision-making than their posterior counterparts (95% CI LOR: pdMCC [−0.2, 0.3], adMCC [0.3, 0.8], pvMCC [−0.2, 0.4], avMCC [0.6, 1.1]).

In the anterior zone (Fig. 4, bottom right), activity across all three subregions was significantly predicted by episodic memory and social processing; however, the association with social processing was maximal for dmPFC (A1) (95% CI LOR: dmPFC [1.3, 1.7], pgACC [0.7, 1], vmPFC [0.6, 1]). In contrast, the reverse was true for reward and decision-making; we observed a gradient such that the association with reward and fear was greatest going ventrally, reaching a maximum in vmPFC (A3) (95% CI LOR: reward: dmPFC [−0.4, 0.3], pgACC [0.5, 1], vmPFC [1.2, 1.7]; fear: dmPFC [−0.4, 0.3], pgACC [0.2, 0.7], vmPFC [0.8, 1.3]).

### Discussion

In the current study, we identified and functionally characterized regions of the MFC by applying a data-driven approach to a large-scale database of  $\sim 10,000$  fMRI studies. We defined regions



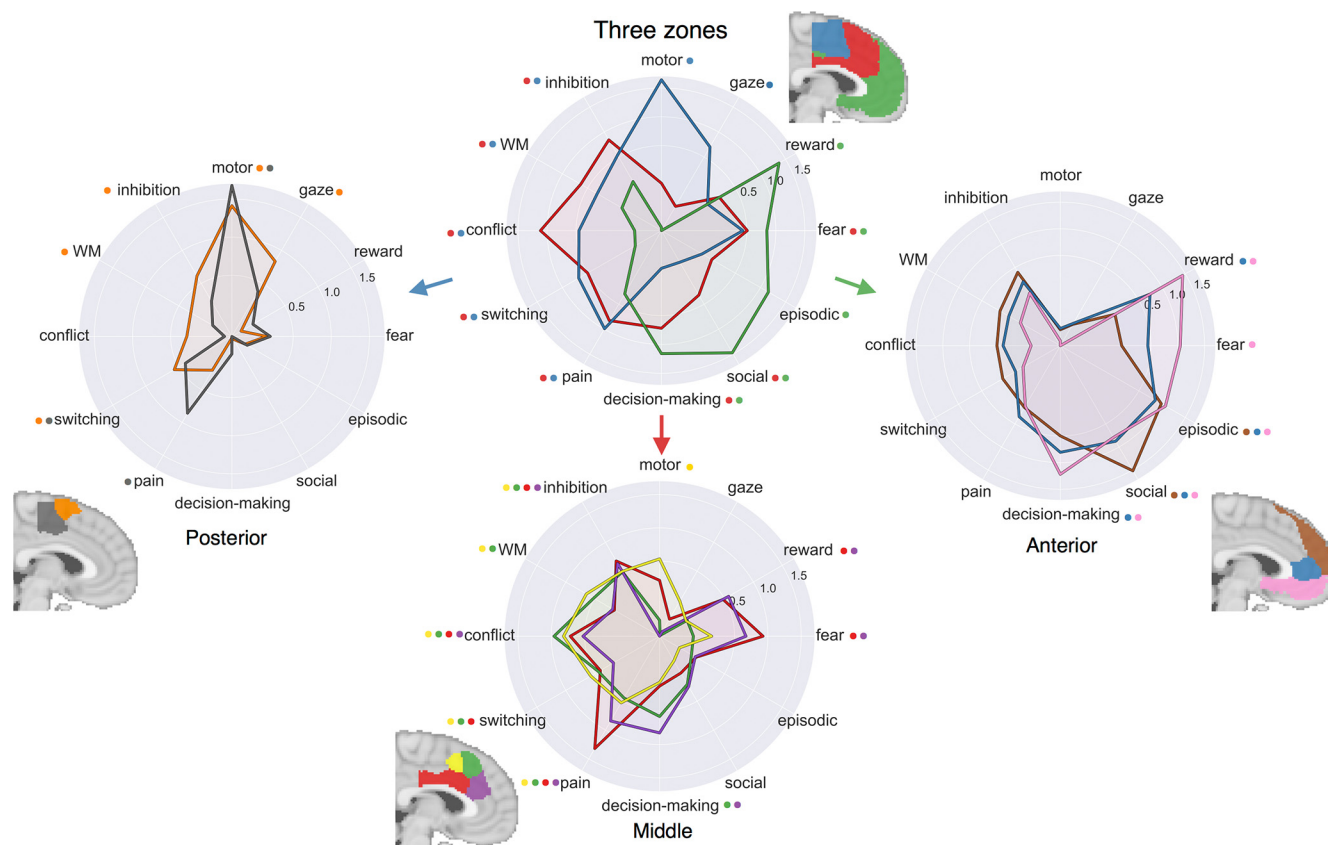


**Figure 4.** Functional preference profiles of MFC clusters. Each cluster was profiled to determine which psychological concepts best predicted its activation. Top, Each of the three functional zones we identified showed distinct functional profiles with broad shifts across cognitive domains. Bottom, Within each zone, subregions showed fine-grained shifts in function. Strength of association is measured in LOR, and permutation-based significance ( $p < 0.001$ ) is indicated next to each psychological concept by color-coded dots corresponding to each region.

on the basis of differences in coactivation patterns across a wide variety of psychological manipulations, a more direct measure of function than morphology or connectivity. We identified three broad zones arranged along the rostrocaudal axis that further fractionated into 2–4 subregions. Finally, we used multivariate classification analyses to identify the psychological topics most strongly predictive of activity in each region, revealing broad shifts in function between the three broad zones and more fine-grained differences between subregions within each zone. In the following sections, we discuss theoretical implications for each zone as well as future challenges.

#### Posterior zone

Posterior MFC spanned various regions previously associated with motoric function, such as SMA, pre-SMA, and motor cingulate zones. This zone further fractionated into a posterior and anterior cluster similarly to cytoarchitectonic (Vorobiev et al., 1998) and connectivity parcellations (Johansen-Berg et al., 2004; Kim et al., 2010). As a whole, posterior MFC was primarily associated with motor function and coactivated with key motor regions, such as primary motor cortex and thalamus. However, SMA (P1) showed a greater association with pain processing and greater coactivation with key pain regions, such as SII and thalamus, suggesting that this region may be important for initiating movements in response to pain. In contrast, pre-SMA (P2) showed a stronger association with cognitive control and coactivated with regions important for goal-directed cognition (e.g., DLPFC, aIns). These results are generally consistent with a large line of work suggesting that pre-SMA is responsible for more

complex motor actions that presumably require cognitive control (Picard and Strick, 1996).

#### Middle zone

The middle MFC zone spanned portions of the cingulate and paracingulate gyri consistent with existing definitions of MCC (Vogt, 2016). In contrast to claims of pain selectivity in MCC (Lieberman and Eisenberger, 2015), all four middle subregions were associated with pain and cognitive control. This finding is broadly consistent with adaptive control hypotheses, which postulate that MCC integrates negative affective signals with cognitive control to optimize actions in the face of action-outcome uncertainty (Shackman et al., 2011; Cavanagh and Shackman, 2015). However, the present results additionally suggest functional differences between subregions of MCC. Notably, both dorsal MCC clusters were more strongly associated with WM and showed greater coactivation with other cognitive control regions, whereas ventral MCC was more strongly associated with affect and coactivated more strongly with subcortical regions, such as amygdala and striatum. Importantly, ventral MCC was associated not only with negative affect and pain, but also reward. Thus, the present results suggest that ventral aspects of MCC may incorporate low-level affective signals into cognitive control, whereas dorsal MCC may be more important for aspects of cognitive motor control that require WM or resolving interference. Finally, we also observed that both anterior MCC clusters were more strongly associated with decision-making than posterior clusters, consistent with theories that incorporate reward-driven

decision-making processes into the optimization of cognitive control (Brown and Braver, 2005; Alexander and Brown, 2011).

### Anterior zone

Anterior MFC exhibited a distinct functional profile with strong associations with affect, decision-making, social cognition, and episodic memory, accompanied by coactivation with the default network. Yet, our results suggest that anterior MFC zone is not a unitary area, and fractionated into functionally differentiable subregions. dmPFC (A1) was most strongly associated with social processing, consistent with studies linking dmPFC to social perception and self-referential thought (Mitchell et al., 2005) and consistent with its robust coactivation with TPJ, a region hypothesized to be important for mentalizing (Baumgartner et al., 2012; Denny et al., 2012). pgACC (A2) showed a less specific functional pattern, showing moderate associations with both affective processes and decision-making, perhaps consistent with descriptions of a default network “hub” region in mPFC (Andrews-Hanna et al., 2010; van den Heuvel and Sporns, 2013). Finally, vmPFC (A3) was primarily associated with affective processes, such as reward and fear, consistent with its robust subcortical coactivation. Although some have characterized vmPFC as a “valuation” system (Lebreton et al., 2009), our results suggest that vmPFC is equally important for other affective processes, such as fear. Thus, vmPFC may play a more general role of incorporating subcortical affective signals into cortex, whereas more dorsal regions contextualize this affective information (Roy et al., 2012).

### Future challenges

Although the present results provide valuable insights into the functional neuroanatomy of MFC, a number of important challenges remain for future research. Although the present analyses revealed distinct functional profiles for each region in MFC, it is notable that no region was selectively activated by a single psychological concept. This functional diversity is evident in that at least two distinct topics were significantly associated with each cluster and our classifier’s poor ability to predict activation using only the single most strongly associated topic for each cluster. These results suggest a complex many-to-many mapping between brain regions and cognitive processes, in contrast to recent claims of functional selectivity in MFC (Lieberman and Eisenberger, 2015; compare Wager et al., 2016). This heterogeneity is consistent with an enormous wealth of electrophysiological data demonstrating that virtually all areas of association cortex contain distinct, but overlapping, neuron populations with heterogeneous functional profiles (Shidara and Richmond, 2002; Sikes et al., 2008; Kvitsiani et al., 2013).

Although the present results provide a comprehensive snapshot of MFC function, many have argued that brain regions dynamically assume different roles (Shackman et al., 2015) and modulate their connectivity as a function of task demands (Cole et al., 2014; Mattar et al., 2015). Moreover, MCC is likely to be among the most heterogeneous brain regions (Anderson et al., 2013) as evidenced by its very high activation rate (Nelson et al., 2010; Yarkoni et al., 2011). Thus, because the functional coactivation profiles presented here represent averages across tasks, they may mask task-dependent coactivation structure. For example, it is possible that ventral MCC coactivates more strongly with the amygdala during “fear” but coactivates with posterior insula during “pain.” An interesting avenue of future research will be to precisely characterize how coactivation and functional patterns of MFC change as a function of context through large-scale meta-analysis.

Moreover, although our parcellation was moderately consistent with boundaries based on cytoarchitecture and connectivity (e.g., the distinction between SMA and pre-SMA), we observed several discrepancies. For example, we did not identify separate cingulate motor zones (Picard and Strick, 1996), suggesting morphologically distinct regions can coactivate similarly to support high-level psychological function (e.g., “motor function”). Systematic modeling of the relationship between anatomy and task evoked activation, similarly to existing models linking resting state and anatomical connectivity (Goñi et al., 2014), is needed to better understand the nature of such discrepancies.

The present report also provides the ability to generate hypotheses that can be more carefully tested in future studies using the candidate psychological functions discussed here. For example, our result suggests that ventral MCC had a higher association with affect than dorsal MCC. However, given the wide intersubject variability in paracingulate anatomy (Paus et al., 1996), it would be prudent to explore this suggestion in a single sample with subject-level anatomical registration. This hypothesis might also be explored by large-scale meta-analyses that combine functional and anatomical data to more precisely localize activity to detailed anatomical variation. Moreover, the present findings can improve the development of future multivariate classifiers by providing better prior information as to the regions that may specifically predict psychological states (e.g., Wager et al., 2013).

Finally, there are several limitations of Neurosynth that can be addressed in future research. First, the topic model we use is data-derived from the semantic content of papers. Although these topics provide a substantial improvement over term-based meta-analysis (Poldrack et al., 2012b), these topics are still based purely on the frequency with which terms appear in the abstracts of articles and are not able to capture more complex semantic structures. The adoption of a standardized ontology of psychological concepts and tasks, such as the Cognitive Atlas (Poldrack et al., 2011), will greatly improve the ability of future meta-analyses to discriminate more fine-grained theories. Second, the quality of activation data in Neurosynth is inherently limited because of its automatically generated nature. Although previous validation analyses have shown that these limitations are unlikely to contribute systematic biases (Yarkoni et al., 2011), coordinate-based meta-analyses are generally limited compared with their image-based counterparts (Salimi-Khorshidi et al., 2009). Sharing of statistical images in databases, such as NeuroVault (Gorgolewski et al., 2015), will greatly improve the fidelity of future meta-analyses.

In conclusion, in the present study, we provide a comprehensive functional map of the human MFC using unbiased data-driven methods. Although the anatomy of this area has been extensively studied, the present study more directly identified putative subregions with distinct functional profiles across a wide variety of psychological states. The present results can serve as a foundation to generate and test more fine-grained hypotheses in future studies.

### Notes

Supplemental material for this article is available at <https://github.com/adelaavega/neurosynth-mfc>. Code and data to replicate these analyses on any given brain region at any desired spatial granularity. This material has not been peer reviewed.

### References

Alexander WH, Brown JW (2011) Medial prefrontal cortex as an action-outcome predictor. *Nat Neurosci* 14:1338–1344. CrossRef Medline



- Amunts K, Zilles K (2015) Architectonic mapping of the human brain beyond Brodmann. *Neuron* 88:1086–1107. [CrossRef Medline](#)
- Anderson ML, Kinnison J, Pessoa L (2013) Describing functional diversity of brain regions and brain networks. *Neuroimage* 73:50–58. [CrossRef Medline](#)
- Andrews-Hanna JR, Reidler JS, Sepulcre J, Poulin R, Buckner RL (2010) Functional-anatomic fractionation of the brain's default network. *Neuron* 65:550–562. [CrossRef Medline](#)
- Andrews-Hanna JR (2012) The brain's default network and its adaptive role in internal mentation. *Neuroscientist* 18:251–270. [CrossRef Medline](#)
- Androutsopoulos I, Koutsias J, Chandrinou KV (2000) An evaluation of naive bayesian anti-spam filtering (Potamias G, Moustakis V, van Someren M, eds), pp 9–17. *Proceedings of the workshop on Machine Learning in the New Information Age, Barcelona, Spain.*
- Baumgartner T, Götze L, Gügler R, Fehr E (2012) The mentalizing network orchestrates the impact of parochial altruism on social norm enforcement. *Hum Brain Mapp* 33:1452–1469. [CrossRef Medline](#)
- Beckmann M, Johansen-Berg H, Rushworth MF (2009) Connectivity-based parcellation of human cingulate cortex and its relation to functional specialization. *J Neurosci* 29:1175–1190. [CrossRef Medline](#)
- Blei DM, Ng AY, Jordan MI (2003) Latent dirichlet allocation. *J Machine Learn Res* 3:993–1022.
- Botvinick M, Nystrom LE, Fissell K, Carter CS, Cohen JD (1999) Conflict monitoring versus selection-for-action in anterior cingulate cortex. *Nature* 402:179–181. [CrossRef Medline](#)
- Brown JW, Braver TS (2005) Learned predictions of error likelihood in the anterior cingulate cortex. *Science* 307:1118–1121. [CrossRef Medline](#)
- Carter RM, Huettel SA (2013) A nexus model of the temporal-parietal junction. *Trends Cogn Sci* 17:328–336. [CrossRef Medline](#)
- Cavanagh JF, Shackman AJ (2015) Frontal midline theta reflects anxiety and cognitive control: meta-analytic evidence. *J Physiol Paris* 109:3–15. [CrossRef Medline](#)
- Chang LJ, Yarkoni T, Khaw MW, Sanfey AG (2013) Decoding the role of the insula in human cognition: functional parcellation and large-scale reverse inference. *Cereb Cortex* 23:739–749. [CrossRef Medline](#)
- Cole MW, Bassett DS, Power JD, Braver TS, Petersen SE (2014) Intrinsic and task-evoked network architectures of the human brain. *Neuron* 83:238–251. [CrossRef Medline](#)
- Critchley HD, Mathias CJ, Josephs O, O'Doherty J, Zanini S, Dewar BK, Cipolotti L, Shallice T, Dolan RJ (2003) Human cingulate cortex and autonomic control: converging neuroimaging and clinical evidence. *Brain* 126:2139–2152. [CrossRef Medline](#)
- Denny BT, Kober H, Wager TD, Ochsner KN (2012) A meta-analysis of functional neuroimaging studies of self- and other judgments reveals a spatial gradient for mentalizing in medial prefrontal cortex. *J Cogn Neurosci* 24:1742–1752. [CrossRef Medline](#)
- Eickhoff SB, Paus T, Caspers S, Grosbras MH, Evans AC, Zilles K, Amunts K (2007) Assignment of functional activations to probabilistic cytoarchitectonic areas revisited. *Neuroimage* 36:511–521. [CrossRef Medline](#)
- Eickhoff SB, Thirion B, Varoquaux G, Bzdok D (2015) Connectivity-based parcellation: critique and implications. *Hum Brain Mapp* 36:4771–4792. [CrossRef Medline](#)
- Etkin A, Egner T, Kalisch R (2011) Emotional processing in anterior cingulate and medial prefrontal cortex. *Trends Cogn Sci* 15:85–93. [CrossRef Medline](#)
- Goñi J, van den Heuvel MP, Avena-Koenigsberger A, Velez de Mendizabal N, Betzel RF, Griffa A, Hagmann P, Corominas-Murtra B, Thiran JP, Sporns O (2014) Resting-brain functional connectivity predicted by analytic measures of network communication. *Proc Natl Acad Sci U S A* 111:833–838. [CrossRef Medline](#)
- Gorgolewski KJ, Varoquaux G, Rivera G, Schwarz Y, Ghosh SS, Maumet C, Sochat VV, Nichols TE, Poldrack RA, Poline JB, Yarkoni T, Margulies DS (2015) NeuroVault.org: a web-based repository for collecting and sharing unthresholded statistical maps of the human brain. *Front Neuroinform* 9:8. [CrossRef Medline](#)
- Hare TA, Camerer CF, Rangel A (2009) Self-control in decision-making involves modulation of the vmPFC valuation system. *Science* 324:646–648. [CrossRef Medline](#)
- Holroyd CB, Nieuwenhuis S, Yeung N, Nystrom L, Mars RB, Coles MG, Cohen JD (2004) Dorsal anterior cingulate cortex shows fMRI response to internal and external error signals. *Nat Neurosci* 7:497–498. [CrossRef Medline](#)
- Jeni LA, Cohn JF, De La Torre F (2013) Facing imbalanced data recommendations for the use of performance metrics. *Int Conf Affect Comput Intell Interact Workshops* 2013:245–251. [CrossRef Medline](#)
- Johansen-Berg H, Behrens TE, Robson MD, Drobniak I, Rushworth MF, Brady JM, Smith SM, Higham DJ, Matthews PM (2004) Changes in connectivity profiles define functionally distinct regions in human medial frontal cortex. *Proc Natl Acad Sci U S A* 101:13335–13340. [CrossRef Medline](#)
- Kennerley SW, Sakai K, Rushworth MF (2004) Organization of action sequences and the role of the pre-SMA. *J Neurophysiol* 91:978–993. [CrossRef Medline](#)
- Kim JH, Lee JM, Jo HJ, Kim SH, Lee JH, Kim ST, Seo SW, Cox RW, Na DL, Kim SI, Saad ZS (2010) Defining functional SMA and pre-SMA subregions in human MFC using resting state fMRI: functional connectivity-based parcellation method. *Neuroimage* 49:2375–2386. [CrossRef Medline](#)
- Kober H, Barrett LF, Joseph J, Bliss-Moreau E, Lindquist K, Wager TD (2008) Functional grouping and cortical-subcortical interactions in emotion: a meta-analysis of neuroimaging studies. *Neuroimage* 42:998–1031. [CrossRef Medline](#)
- Kvitsiani D, Ranade S, Hangya B, Taniguchi H, Huang JZ, Kepecs A (2013) Distinct behavioural and network correlates of two interneuron types in prefrontal cortex. *Nature* 498:363–366. [CrossRef Medline](#)
- Lebreton M, Jorge S, Michel V, Thirion B, Pessiglione M (2009) An automatic valuation system in the human brain: evidence from functional neuroimaging. *Neuron* 64:431–439. [CrossRef Medline](#)
- Leek EC, Johnston SJ (2009) Functional specialization in the supplementary motor complex. *Nat Rev Neurosci* 10:78. [CrossRef Medline](#)
- Lieberman MD, Eisenberger NI (2015) The dorsal anterior cingulate cortex is selective for pain: results from large-scale reverse inference. *Proc Natl Acad Sci U S A* 112:15250–15255. [CrossRef Medline](#)
- Lindquist KA, Wager TD, Kober H, Bliss-Moreau E, Barrett LF (2012) The brain basis of emotion: a meta-analytic review. *Behav Brain Sci* 35:121–143. [CrossRef Medline](#)
- Mackey S, Petrides M (2014) Architecture and morphology of the human ventromedial prefrontal cortex. *Eur J Neurosci* 40:2777–2796. [CrossRef Medline](#)
- Mattar MG, Cole MW, Thompson-Schill SL, Bassett DS (2015) A functional cartography of cognitive systems. *PLoS Comput Biol* 11:e1004533. [CrossRef Medline](#)
- Milad MR, Quirk GJ, Pitman RK, Orr SP, Fischl B, Rauch SL (2007) A role for the human dorsal anterior cingulate cortex in fear expression. *Biol Psychiatry* 62:1191–1194. [CrossRef Medline](#)
- Milham MP, Banich MT, Webb A, Barad V, Cohen NJ, Wszalek T, Kramer AF (2001) The relative involvement of anterior cingulate and prefrontal cortex in attentional control depends on nature of conflict. *Cogn Brain Res* 12:467–473. [CrossRef Medline](#)
- Mitchell JP, Banaji MR, Macrae CN (2005) The link between social cognition and self-referential thought in the medial prefrontal cortex. *J Cogn Neurosci* 17:1306–1315. [CrossRef Medline](#)
- Nelson SM, Dosenbach NU, Cohen AL, Wheeler ME, Schlaggar BL, Petersen SE (2010) Role of the anterior insula in task-level control and focal attention. *Brain Struct Funct* 214:669–680. [CrossRef Medline](#)
- Neubert FX, Mars RB, Thomas AG, Sallet J, Rushworth MF (2014) Comparison of human ventral frontal cortex areas for cognitive control and language with areas in monkey frontal cortex. *Neuron* 81:700–713. [CrossRef Medline](#)
- Palomero-Gallagher N, Zilles K, Schleicher A, Vogt BA (2013) Cyto- and receptor architecture of area 32 in human and macaque brains. *J Comp Neurol* 521:3272–3286. [CrossRef Medline](#)
- Palomero-Gallagher N, Eickhoff SB, Hoffstaedt F, Schleicher A, Mohlberg H, Vogt BA, Amunts K, Zilles K (2015) Functional organization of human subgenual cortical areas: relationship between architectonical segregation and connectional heterogeneity. *Neuroimage* 115:177–190. [CrossRef Medline](#)
- Paus T, Tomaiuolo F, Otaky N, MacDonald D, Petrides M, Atlas J, Morris R, Evans AC (1996) Human cingulate and paracingulate sulci: pattern, variability, asymmetry, and probabilistic map. *Cereb Cortex* 6:207–214. [CrossRef Medline](#)
- Pedregosa F, Varoquaux G, Gamfort A, Michel V, Thirion B, Grisel O, Blondel M, Prettenhofer P (2011) Scikit-learn: machine learning in python. *J Machine Learn Res* 12:2825–2830.

- Picard N, Strick PL (1996) Motor areas of the medial wall: a review of their location and functional activation. *Cereb Cortex* 6:342–353. [CrossRef Medline](#)
- Poldrack RA (2006) Can cognitive processes be inferred from neuroimaging data? *Trends Cogn Sci* 10:59–63. [CrossRef Medline](#)
- Poldrack RA, Yarkoni T (2016) From brain maps to cognitive ontologies: informatics and the search for mental structure. *Annu Rev Psychol* 67:587–612. [CrossRef Medline](#)
- Poldrack RA, Kittur A, Kalar D, Miller E, Seppa C, Gil Y, Parker DS, Sabb FW, Bilder RM (2011) The cognitive atlas: toward a knowledge foundation for cognitive neuroscience. *Front Neuroinform* 5:17. [CrossRef Medline](#)
- Poldrack RA, Mumford JA, Schonberg T, Kalar D, Barman B, Yarkoni T (2012a) Discovering relations between mind, brain, and mental disorders using topic mapping. *PLoS Comput Biol* 8:e1002707. [CrossRef Medline](#)
- Poldrack RA, Mumford JA, Schonberg T, Kalar D, Barman B, Yarkoni T (2012b) Discovering relations between mind, brain, and mental disorders using topic mapping. *PLoS Comput Biol* 8:e1002707. [CrossRef Medline](#)
- Robinson JL, Laird AR, Glahn DC, Lovullo WR, Fox PT (2010) Metaanalytic connectivity modeling: delineating the functional connectivity of the human amygdala. *Hum Brain Mapp* 31:173–184. [CrossRef Medline](#)
- Roland PE, Larsen B, Lassen NA, Skinhoj E (1980) Supplementary motor area and other cortical areas in organization of voluntary movements in man. *J Neurophysiol* 43:118–136. [Medline](#)
- Rolls ET, O'Doherty J, Kringelbach ML, Francis S, Bowtell R, McGlone F (2003) Representations of pleasant and painful touch in the human orbitofrontal and cingulate cortices. *Cereb Cortex* 13:308–317. [CrossRef Medline](#)
- Roy M, Shohamy D, Wager TD (2012) Ventromedial prefrontal-subcortical systems and the generation of affective meaning. *Trends Cogn Sci* 16:147–156. [CrossRef Medline](#)
- Salimi-Khorshidi G, Smith SM, Keltner JR, Wager TD, Nichols TE (2009) Meta-analysis of neuroimaging data: a comparison of image-based and coordinate-based pooling of studies. *Neuroimage* 45:810–823. [CrossRef Medline](#)
- Sallet J, Mars RB, Noonan MP, Neubert FX, Jbabdi S, O'Reilly JX, Filippini N, Thomas AG, Rushworth MF (2013) The organization of dorsal frontal cortex in humans and macaques. *J Neurosci* 33:12255–12274. [CrossRef Medline](#)
- Shackman AJ, Salomons TV, Slagter HA, Fox AS, Winter JJ, Davidson RJ (2011) The integration of negative affect, pain and cognitive control in the cingulate cortex. *Nat Rev Neurosci* 12:154–167. [CrossRef Medline](#)
- Shackman AJ, Fox AS, Seminowicz DA (2015) The cognitive-emotional brain: opportunities and challenges for understanding neuropsychiatric disorders. *Behav Brain Sci* 38:e86. [CrossRef Medline](#)
- Shenhav A, Botvinick MM, Cohen JD (2013) The expected value of control: an integrative theory of anterior cingulate cortex function. *Neuron* 79:217–240. [CrossRef Medline](#)
- Shidara M, Richmond BJ (2002) Anterior cingulate: single neuronal signals related to degree of reward expectancy. *Science* 296:1709–1711. [CrossRef Medline](#)
- Sikes RW, Vogt LJ, Vogt BA (2008) Distribution and properties of visceral nociceptive neurons in rabbit cingulate cortex. *Pain* 135:160–174. [CrossRef Medline](#)
- Smith SM, Fox PT, Miller KL, Glahn DC, Fox PM, Mackay CE, Filippini N, Watkins KE, Toro R, Laird AR, Beckmann CF (2009) Correspondence of the brain's functional architecture during activation and rest. *Proc Natl Acad Sci U S A* 106:13040–13045. [CrossRef Medline](#)
- Spreng RN, Grady CL (2010) Patterns of brain activity supporting autobiographical memory, prospection, and theory of mind, and their relationship to the default mode network. *J Cogn Neurosci* 22:1112–1123. [CrossRef Medline](#)
- Stalnaker TA, Cooch NK, Schoenbaum G (2015) What the orbitofrontal cortex does not do. *Nat Neurosci* 18:620–627. [CrossRef Medline](#)
- Thirion B, Varoquaux G, Dohmatob E, Poline JB (2014) Which fMRI clustering gives good brain parcellations? *Front Neurosci* 8:167. [CrossRef Medline](#)
- Toro R, Fox PT, Paus T (2008) Functional coactivation map of the human brain. *Cereb Cortex* 18:2553–2559. [CrossRef Medline](#)
- van den Heuvel MP, Sporns O (2013) Network hubs in the human brain. *Trends Cogn Sci* 17:683–696. [CrossRef Medline](#)
- Varoquaux G, Thirion B (2014) How machine learning is shaping cognitive neuroimaging. *Gigascience* 3:28. [CrossRef Medline](#)
- Vogt BA (2005) Pain and emotion interactions in subregions of the cingulate gyrus. *Nat Rev Neurosci* 6:533–544. [CrossRef Medline](#)
- Vogt BA (2016) Midcingulate cortex: structure, connections, homologies, functions and diseases. *J Chem Neuroanat* 74:28–46. [CrossRef Medline](#)
- Vogt BA, Vogt L (2003) Cytology of human dorsal midcingulate and supplementary motor cortices. *J Chem Neuroanat* 26:301–309. [CrossRef Medline](#)
- Vorobiev V, Govoni P, Rizzolatti G, Matelli M, Luppino G (1998) Parcellation of human mesial area 6: cytoarchitectonic evidence for three separate areas. *Eur J Neurosci* 10:2199–2203. [CrossRef Medline](#)
- Wager TD, Davidson ML, Hughes BL, Lindquist MA, Ochsner KN (2008) Prefrontal-subcortical pathways mediating successful emotion regulation. *Neuron* 59:1037–1050. [CrossRef Medline](#)
- Wager TD, Atlas LY, Lindquist MA, Roy M, Woo CW, Kross E (2013) An fMRI-based neurologic signature of physical pain. *N Engl J Med* 368:1388–1397. [CrossRef Medline](#)
- Wager TD, Atlas LY, Botvinick MM, Chang LJ, Coghill RC, Davis KD, Iannetti GD, Poldrack RA, Shackman AJ, Yarkoni T (2016) Pain in the ACC? *Proc Natl Acad Sci U S A* 113:E2474–E2475. [CrossRef Medline](#)
- Yarkoni T, Poldrack RA, Nichols TE, Van Essen DC, Wager TD (2011) Large-scale automated synthesis of human functional neuroimaging data. *Nat Methods* 8:665–670. [CrossRef Medline](#)
- Zilbovicius M, Meresse I, Chabane N, Brunelle F, Samson Y, Boddaert N (2006) Autism, the superior temporal sulcus and social perception. *Trends Neurosci* 29:359–366. [CrossRef Medline](#)